DLINE JOURNALS

Electronic Devices

Print ISSN: 2278 – 6422
Online ISSN: 2278 – 6430

ED 2024; 13(2)
https://doi.org/10.6025/ed/2024/13/2/67-73

Coherence Maps for SAR Image Pairs Processing

Nina S. Vinogradova and Andrey V. Sosnovsky
Ural Federal University, Yekaterinburg
Mira st., 19, Russia
n.s.vinogradova@urfu.ru

ABSTRACT

This paper discusses the methods for creating coherence maps for processing SAR image pairs. It outlines the acceptable range of coherence values for the averaging window. Based on these findings, the paper also introduces a method for enhancing map coherence. The SAR interferogram calculation using this enhanced method is carried out. The paper demonstrates an improvement in accuracy compared to traditional techniques.

Received: 11 April 2024
Revised: 8 July 2024
Accepted: 10 July 2024

Keywords: Image Analysis, Coherence Map, Insar Processing, Computer Simulation

1. Introduction

Coherence map is an image of the SAR pair correlation coefficients field. It gives information about deviation degree of the absolute phase from its true value. Such deviation may be caused by the phase noise, a surface variability, and the stability of the radio signal reflected from various parts of the Earth surface [1]. Coherence map may be useful for a wide range of problems solved by systems of radar sense remote data such as urban planning, emergencies monitoring, and issues of environmental protection [2, 3]. It allows one to view the characteristics of the satellite system, atmospheric and weather conditions, the properties of the radar signal and the Earth surface, and, ultimately, the quality of products created on the basis of SAR data, such as DEM (digital elevation models) and terrain displacement maps [4-6]. According to the definition, the brightness value of the coherence map elements may take values in the range [0, 1] only. The value 0 corresponds to complete decorrelation, the value 1 corresponds to absolute coherence of the corresponding elements of the Earth's surface. It is conventionally accepted to classify the elements of the coherence map into three classes: zones with low coherence corresponding to dark areas, zones with high coherence corresponding to light regions, and zones with intermediate coherence values corresponding to gray areas [7, 8].

The coherence map development is performed at the stage of the SAR interferogram creating. According to the traditional technique, value of each element is calculated as the correlation coefficient between the values of the first and

second SAR images in the pair. The classical method of coherence map development is based on multiplying the first (reference) image of the interferometric pair by the second (auxiliary) one that is complex-conjugate to itself [1, 5, 9]

$$\hat{\gamma} = \frac{|\sum_{x=0}^{M-1}\sum_{y=0}^{N-1} Z_1(x,y)\cdot Z_2^*(x,y)|}{\sqrt{\sum_{x=0}^{M-1}\sum_{y=0}^{N-1}|Z_1(x,y)|^2\cdot\sum_{x=0}^{M-1}\sum_{y=0}^{N-1}|Z_2(x,y)|^2}},$$

where Z_1, Z_2 are the radar images of the reference and auxiliary signals respectively, M, N are the dimensions of the averaging region size, * is the complex conjugation operator.

Despite the fact that the correlation function has been thoroughly studied in details [10, 11], the issue of its usage for two-dimensional digital signals obtained by radar interferometric survey is still unclear.

2. Coherence Magnitude Estimation Analysis

Firstly, it is necessary to obtain the minimum averaging region size N with is used during the coherence map development. The plot of dependence of the bias of estimate of coherence magnitude d^ at zero correlation on the averaging region size is constructed. The size N in terms of expression (1) is similar to the sample size used in calculating the correlation coefficient. Due to the finiteness of the sample, a bias of the correlation estimate may occur in the coherence map development. The displacement value will increase with decreasing coherence and reach the maximum values at zero. For calculations, the test image corresponding to a at terrain without any relief changes is used. Test images are combined with the Gaussian noise by complex multiplication operation. The range of the averaging window is from 3 to 65 elements. The results are shown in Figure 1.

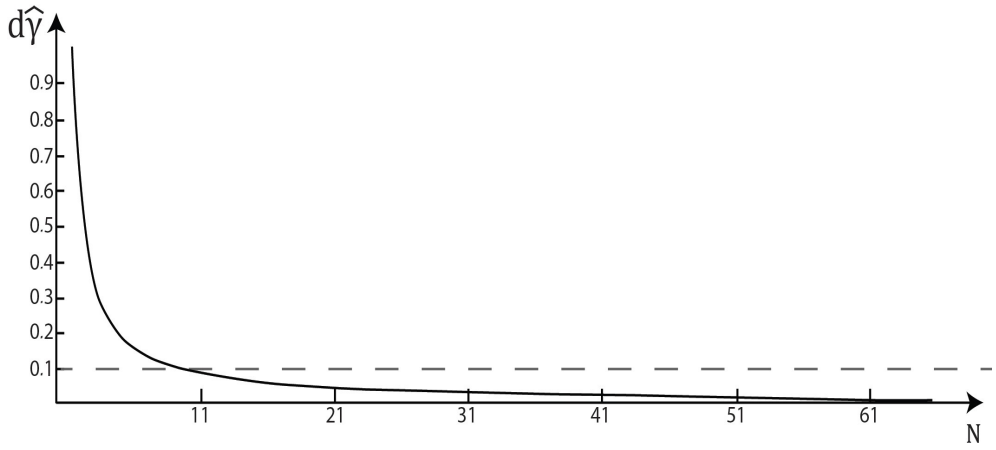

Figure 1. The dependence of bias estimate on coherence magnitude d^ for the size of the averaging region N

As it follows from the figure, the minimum averaging region size is the size of 11 elements for the classical method of coherence map development. Using the smaller one, the bias in the coherence estimate exceeds 0.1. This effect may deeply distort the interpretation of the output product. The dependence has the form of a hyperbolic curve slowly converging to zero value, which corresponds to the classical notions of the significance of estimating the bias from the window size [10].

To analyze the behavior of the estimation using the classical method, the dependence STD of estimate of coherence magnitude on the varied coherence $\sigma_{\hat{\gamma}} = \sigma_{\hat{\gamma}}(\gamma)$ is performed. The

STD estimate changes in the coherence interval from 0 to 1 with step of 0.005. The calculations are made for the averaging region size $11\times11, 19\times19, 27\times27, 35\times35, 43\times43, 51\times51, 67\times67$. Averaging at 600 points is performed. The obtained dependences are presented in Figure 2.

The abscissa axis shows a range from 0 to 0.3 for clarity.

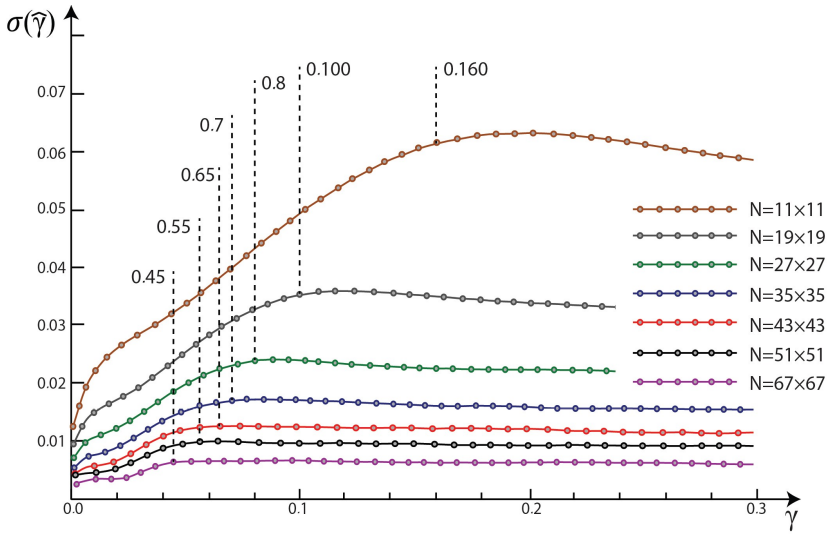

Figure 2. The dependence STD of estimate of coherence magnitude on the varied coherence the positions of the dropping peaks are shown by a vertical dotted line

As it follows from the figure, behavior of the dependence $\sigma_{\hat{\gamma}} = \sigma_{\hat{\gamma}}(\gamma)$ is similar to the lower Rao-

N	d	dp	N	d	dp	N	d	dp
11	0.081	0.160	31	0.030	0.070	51	0.019	0.055
13	0.069	0.145	33	0.028	0.070	53	0.018	0.055
15	0.060	0.130	35	0.027	0.070	55	0.018	0.055
17	0.053	0.115	37	0.025	0.065	57	0.017	0.050
19	0.048	0.100	39	0.024	0.065	59	0.017	0.050
21	0.043	0.095	41	0.023	0.065	61	0.016	0.050
23	0.040	0.090	43	0.022	0.065	63	0.014	0.050
25	0.037	0.085	45	0.021	0.060	65	0.014	0.045
27	0.034	0.080	47	0.020	0.060	67	0.013	0.045
29	0.032	0.075	49	0.020	0.055	69	0.013	0.045

Table 1. The dependence of the dropping peak position dp and bias of estimate of coherence magnitude d on the averaging region size N

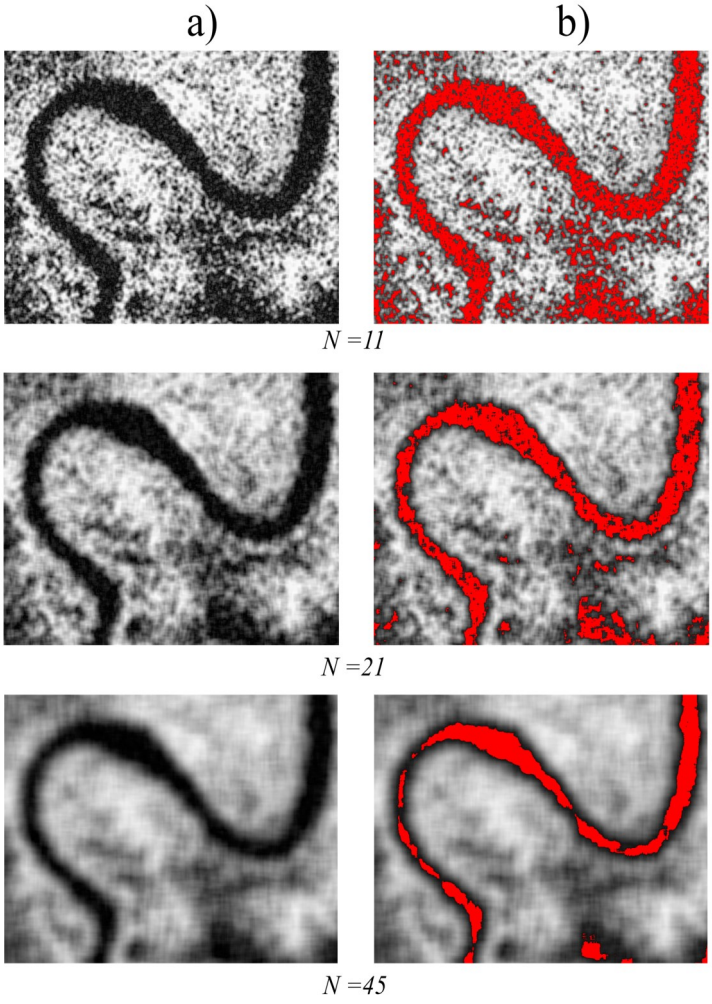

Figure 3. Simulation of the coherence maps of the PCA-pair fragment for different sizes of the averaging window: a) coherence maps; b) regions with a coherence value below dp for a fixed averaging window size

Kramer boundary [10, 12-14]. The discrepancy with the theoretical dependency is due to the fact that the Rao-Cramer formula shows reliable values for sufficiently large sampling values. Also, the dropping peaks are distinctly distinguished at the calculated values, after which the value o thef STD estimate drops sharply to the minimum values. The reason for this is that there is a bias in the STD estimate (Figure 1). Position of the dropping peak depends on the window size: the smaller the window size, the farther from the zero is the peak. This fact is caused by a decrease in the STD estimate of coherence magnitude with increasing sample size. It follows that the range of brightness values on the output coherence map corresponding to the set of coherence values (which are located between the zero and the dropping peak) is incorrect and have to be removed from the output coherence map. A summary of the obtained results is presented in Table 1.

To illustrate the data of Table 1, the coherence map for two images of SAR pair was modeled using the classical expression (1) (the data are taken from [15]). The calculation was carried out with the averaging window sizes 11×11×21×21×45×45. The regions with coherence values below γ_{dp} are sown by color.

As it follows from the Figure 4, during increasing averaging region size, the effective area

of the coherence map increases too. It becomes possible to build a mask of pixels, which are incorrect. At the same time, it should be noted that during increasing averaging region size, the final product details decrease. The present result will be used to improve the interferogram accuracy for the SAR image pair in the tasks of DEM creation.

3. Experimental Results

For interferogram accuracy of obtained products, the STD of absolute phase deviation from a reference DEM was calculated as a quality indicator for the interferometric coherence estimate. The better estimates should give a less- fluctuation decreasing dependence for at least for low- and medium-valued coherences with a possible wider range of both coherence and STD values. The method based on coherence map masking has shown the more accurate result: the range of deviation is wider by 11 percent in comparison with traditional techniques.

The reference DEM covered a territory of 8×5 km, which contained average hills and river valleys. The averaging window size was 15×15, the value of responding dropping peak γ_{dp} was 0.13. Two coherence maps were used for interferogram creation: one was obtained with the traditional method, and another was generated according to the proposed method. The results are shown in Figure 4.

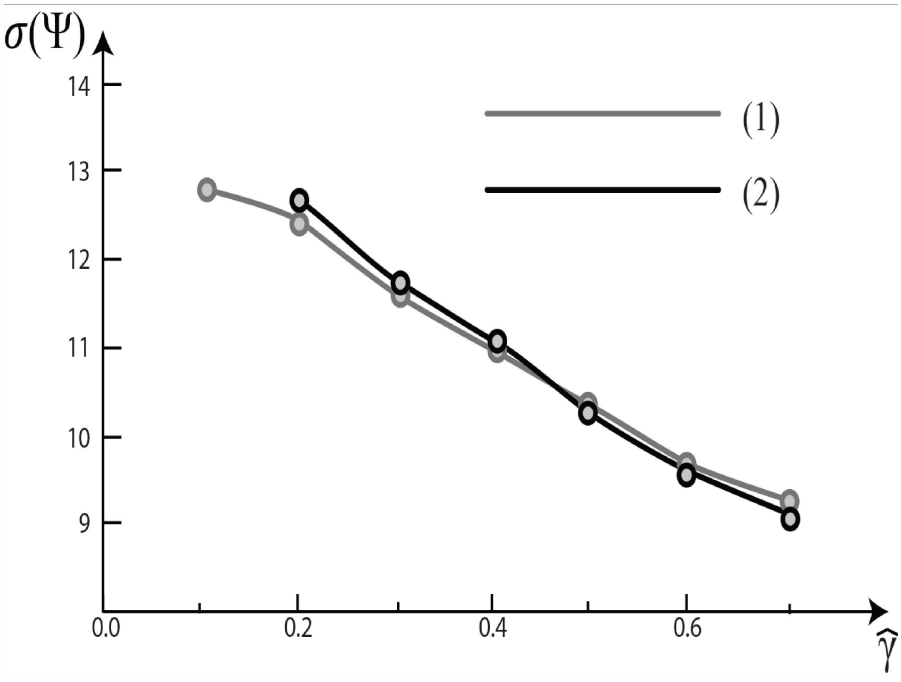

Figure 4. The dependence of phase STD on the coherence magnitude estimation. 1) The one was obtained with traditional method; 2) The one was obtained with coherence map masking

4. Conclusion

The traditional method of the coherence map generation was investigated. Some statistics results related to a classical expression were obtained. The new method of interferogram creation based on dropping peak position was proposed. The method has shown the more accurate result: the range of deviation is wider by 3.8 percent in comparison with traditional techniques.

5. Acknowledgment

This work was supported by the Ural Federal University's Center of Excellence in \Geoinformation technologies and geophysical data complex interpretation methods" (according to the Act 211 Government of the Russian Federation, 0 contract 02.A03.21.0006)

References

[1] Monti Guarnieri, A., Guccione, P., Pasquali, P Desnos, Y. L. (2003). Multi-mode ENVISAT ASAR interferometry: Techniques and preliminary results. *IEE Proceedings - Radar, Sonar and Navigation*, 150(3), 193–200.

[2] Arciniegas, G. A., Bijker, W., Kerle, N Tolpekin, V. A. (2007). Coherence- and amplitude-based analysis of seismogenic damage in Bam, Iran, using ENVISAT ASAR data. *IEEE Transactions on Geoscience and Remote Sensing*, 45(6), 1571–1581.

[3] Takeuchi, S., Suga, Y. (2000). Detection of urban disaster using InSAR: A case study for the 1999 Great Taiwan earthquake. In *Geoscience and Remote Sensing Symposium, 2000. Proceedings. IGARSS 2000. IEEE 2000 International* (pp. 1201–1224).

[4] Askne, J Hagberg, J. O. (1993). Potential of interferometric SAR for classification of land surfaces. In *Proc. Int. Geoscience and Remote Sensing Symp. (IGARSS '93)* (pp. 985–987).

[5] Gens, R van Genderen, J. L. (1996). SAR interferometry: Issues and techniques. *International Journal of Remote Sensing*, 17, 1803–1835.

[6] Lee, H. (2001). Analysis of topographic decorrelation in SAR interferometry using ratio coherence imagery. *IEEE Transactions on Geoscience and Remote Sensing*, 39(2), 223–232.

[7] Abdelfattah, R Nicolas, J. M. (2005). Coherence estimation from complex coherence map using second kind statistics. In *Intern. Conf. on Image Processing, ICIP'05* (Vol. II, pp. 229–232).

[8] Cattabeni, M., Monti-Guarnieri, A Rocca, F. (1994). Estimation and improvement of coherence in SAR interferograms. In *Geoscience and Remote Sensing Symposium, IGARSS '94. Surface and Atmospheric Remote Sensing: Technologies, Data Analysis and Interpretation* (Vol. 4, pp. 720–722).

[9] Wang, T., Liao, M Perissin, D. (2010). InSAR coherence decomposition analysis. *IEEE Geoscience and Remote Sensing Letters*, 7(1), 156–160.

[10] Goriainov, V. B., Pavlov, I. V., Tsvetkova, G. M., et al. (2001). *Matematika v tekhnicheskom universitete. Iss. XVI. Matematicheskaia statistika*. Bauman Moscow State Technical University.

[11] Levin, B. R. (1968). *Teoreticheskie osnovy statisticheskoi radiotekhniki. Kniga 2*. Sovetskoe Radio, Moscow.

[12] Touzi, R., Lopes, A Vachon, P. W. (1999). Coherence estimation for SAR imagery. *IEEE Transactions on Geoscience and Remote Sensing*, 37(1), 135–149.

[13] Valeev, V. G. (1987). *Pomehoustoi'chivost' radiotekhnicheskikh izmeritel'nykh sistem*. Kirov Ural Polytechnic Institute, Sverdlovsk.

[14] Van Trees, H. L. (1992). *Detection, estimation and modulation theory. P. 1. Detection, estimation and linear modulation theory*. Krieger Publishing Co., Inc., Melbourne, FL, USA.

[15] Sentinel Online. Retrieved from https://sentinel.esa.int

[16] Sosnovsky, A. V., Kobernichenko, V. G., Vinogradova, N. S Tsogtbaatar, O. (2017). InSAR data coherence estimation using 2D fast Fourier transform. In *1st International Workshop on Radio Electronics and Information Technologies, REIT 2017, CEUR Workshop Proceedings* (Vol. 1814, pp. 98–105).